

UDC 669.017.15

## EFFECT OF ELECTRON BEAM TREATMENT ON THE FRACTURE BEHAVIOR OF HIGH-ENTROPY Cr – Mn – Fe – Co – Ni ALLOY

V. E. Gromov,<sup>1</sup> Yu. A. Shlyarova,<sup>1</sup> Yu. F. Ivanov,<sup>2</sup> C. V. Konovalov,<sup>3</sup> and C. V. Vorob'ev<sup>1</sup>Translated from *Metallovedenie i Termicheskaya Obrabotka Metallov*, No. 5, pp. 35 – 39, May, 2022.*Original article submitted December 23, 2021.*

The study investigates a high-entropy non-equiatom alloy of the Co – Cr – Fe – Mn – Ni system obtained using wire-arc additive manufacturing (WAAM) technology and subjected to electron beam irradiation (EBI). The strain curves of alloy samples under tension after fabrication and EBI are analyzed. The structure of the fracture surface of the alloy was studied using scanning electron microscopy. The strength and plasticity of the alloy are shown to decrease with an increase in the energy density of the electron beam. This is assumed to be due to the appearance of defects in the structure of the surface layers as a result of elastic stresses arising during high-speed quenching of samples following thermal exposure to an electron beam.

**Keywords:** high-entropy alloy, Cr – Mn – Fe – Co – Ni, electric arc additive technology, pulsed electron beam, tensile testing, fracture surface structure.

### INTRODUCTION

Over the last two decades, the attention of researchers in physical materials science has been attracted to the study of high-entropy alloys (HEA) [1 – 7], which offer a complex of unique properties not achievable with alloying by conventional methods [8]. The basic idea of high-entropy alloys is that the main elements take the form of simple solid solutions, whose formation causes deformation of the crystal structure to improve the thermodynamic stability of its properties due to differences in the atomic radii of components. The thus-formed high entropy contributes to the creation of alloys with unique properties that are impossible to achieve when using traditional micro-alloying methods [9 – 12].

One of the first studied high-entropy alloys is an alloy of the Co – Cr – Fe – Mn – Ni system, which is able to maintain its face-centred cubic (FCC) structure across a wide temperature range, as well as offering a good balance of strength and plasticity [13]. In [14], it is shown that this alloy has simulta-

neously high strength characteristics at room temperature and viscosity at cryogenic temperature (77 K) as a result of the dominance of twinning as a deformation mechanism. However, the main disadvantage of alloys of the Co – Cr – Fe – Mn – Ni system is their relatively low yield strength at room temperature.

Electron beam irradiation (EBI) is one of the promising methods for conducting surface modification of metallic materials to significantly increase their mechanical properties by optimizing the structure of the surface layer [15]. During irradiation, high-density electron beams cause processes such as high-speed recrystallization, surface smoothing, and annealing to occur in the surface layer over an extremely short period of time [16, 17].

During EBI, ultra-high heating rates (up to  $10^6$  K/sec) of the surface layer occur up to the set temperatures along with cooling due to heat removal into the main volume of the material at speeds of  $1 \times 10^4$  –  $1 \times 10^9$  K/sec. As a result, non-equilibrium submicro- and nano-crystalline structural-phase states are formed in the surface layer.

The purpose of the present work is to study the effect of electron beam processing on the mechanical properties and failure mode of a high-entropy alloy of the Co – Cr – Fe – Mn – Ni system.

<sup>1</sup> Siberian State Industrial University, Novokuznetsk, Russia (e-mail: gromov@physics.sibsiu.ru).

<sup>2</sup> Institute of High-Current Electronics of the Siberian Branch of the Russian Academy of Sciences (ISE SB RAS), Tomsk, Russia.

<sup>3</sup> S. P. Korolev Samara National Research University, Samara, Russia.

## METHODS OF STUDY

A high-entropy alloy (HEA) of the Co – Cr – Fe – Mn – Ni system was investigated. The alloy was manufactured using wire arc additive manufacturing (WAAM) technology [8]. To obtain this alloy, a three-core wire consisting of pure cobalt wire ( $\approx 99.9$  at.% Co) with a diameter of 0.47 mm was used as the starting material; Autrod welding wire 16.95 ( $\approx 65.3$  at.% Fe; 19.6 at.% Co; 7.3 at.% Ni; 1.6 at.% Si; 6.2 at.% Mn), which was previously thinned from  $\varnothing 0.80$  to  $\varnothing 0.74$  mm; Ni80Cr20 chromium-nickel wire with a diameter of 0.4 mm ( $\approx 22.5$  at.% Cr; 1.5 at.% Fe; 72.1 at.% Ni; 0.8 at.% Al; 2.9 at.% Si; 0.2 at.% Mn). The original wires were twisted using a special twisting device. The diameter of the combined Co – Cr – Fe – Mn – Ni system cable was  $\approx 1.25$  mm, with a laying length of 10 mm. The production of HEA samples was carried out by layer-by-layer deposition of the starting material on a 12X18H10T steel substrate using WAAM technology in an inert gas atmosphere ( $\approx 99.99\%$  Ar). The layers were applied according to the following mode: wire feed speed — 13 m/min; voltage — 22 V; traveling speed of burner — 0.1 m/min. The resulting high-entropy alloy parallelepiped billet had dimensions of  $140 \times 20 \times 30$  mm consisting of seven deposited layers in height and four layers in width. Tensile tests were carried out on flat proportional samples in the form of double-sided blades in accordance with GOST 1497–84 [18]. The samples were cut from a massive billet using electroerosion methods. Prior to carrying out the tests, the samples had the following dimensions: thickness — 1.05 mm; width — 4.4 mm; length of the working part — 8.0 mm.

Some of the samples were exposed to EPO irradiation with a high-density electron beam from both sides (the working part) at the SOLO facility, then developed and manufactured at the ISE SB RAS [19]. Irradiation modes were as follows: electron beam energy density — 10, 15, 20, 25, 30 J/cm<sup>2</sup>; beam pulse duration — 50  $\mu$ sec; number of pulses — 3; pulse repetition rate — 0.3 sec<sup>-1</sup>. The irradiation was carried out in an argon medium at a residual pressure of 0.02 Pa. Uniaxial tensile tests of the samples were carried out on the Instron 3369 installation (test speed — 1.2 mm/min; temperature — 22°C); deformation curve recording — automatic.

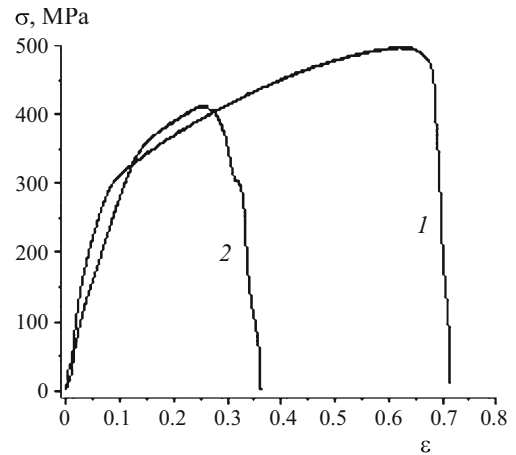


**Fig. 1.** Deformation curves obtained by stretching a high-entropy Cr – Mn – Fe – Co – Ni alloy in the initial state (1) and after irradiation with a pulsed electron beam at  $E_s = 30$  J/cm<sup>2</sup> (2).

## RESULTS AND DISCUSSION

The chemical composition of the HEA is given in Table 1. Analysis of the data according to the ratio of chemical elements shows that the resulting alloy refers to alloys of non-equiatomic composition. In addition, irradiation of the alloy with a pulsed electron beam leads to some redistribution of chemical elements in the surface layer: a decrease in the concentration of iron and nickel and an increase in the concentration of cobalt. No new phases were detected in the HEA following EBI, which indicates the thermal stability of the alloy's crystal lattice.

Mechanical tests of the HEA in the initial and irradiated states, performed by uniaxial stretching of plane proportional samples, showed that in the initial state (before irradiation) the alloy has a high level of plasticity (linear strain exceeds 70%) and strength (tensile strength reaches 500 MPa) (Fig. 1, curve 1). Irradiation of the alloy with a pulsed electron beam in high-speed melting mode and subsequent high-speed crystallization of the surface layer leads to a simultaneous decrease in the strength and ductility characteristics of the material (Fig. 1, curve 2).

Electron microscopic analysis of the fracture surface of the initial samples, along with the viscous patchy character of the fracture (Fig. 2a), revealed the presence of micro-

**TABLE 1.** Chemical composition of high-entropy Cr – Mn – Fe – Co – Ni alloy

State	Content of alloying elements, %				
	Cr	Mn	Fe	Co	Ni
Before irradiation	14.3/15.5	3.0/3.1	38.4/38.9	25.7/24.6	18.6/17.9
After irradiation	14.3/15.5	3.0/3.1	37.8/37.9	27.0/26.0	17.9/17.5

**Note.** 1. The numerator shows the content of elements in mass fractions, in the denominator — in atomic fraction.  
2. The composition of the alloy was determined using x-ray spectroscopy methods.

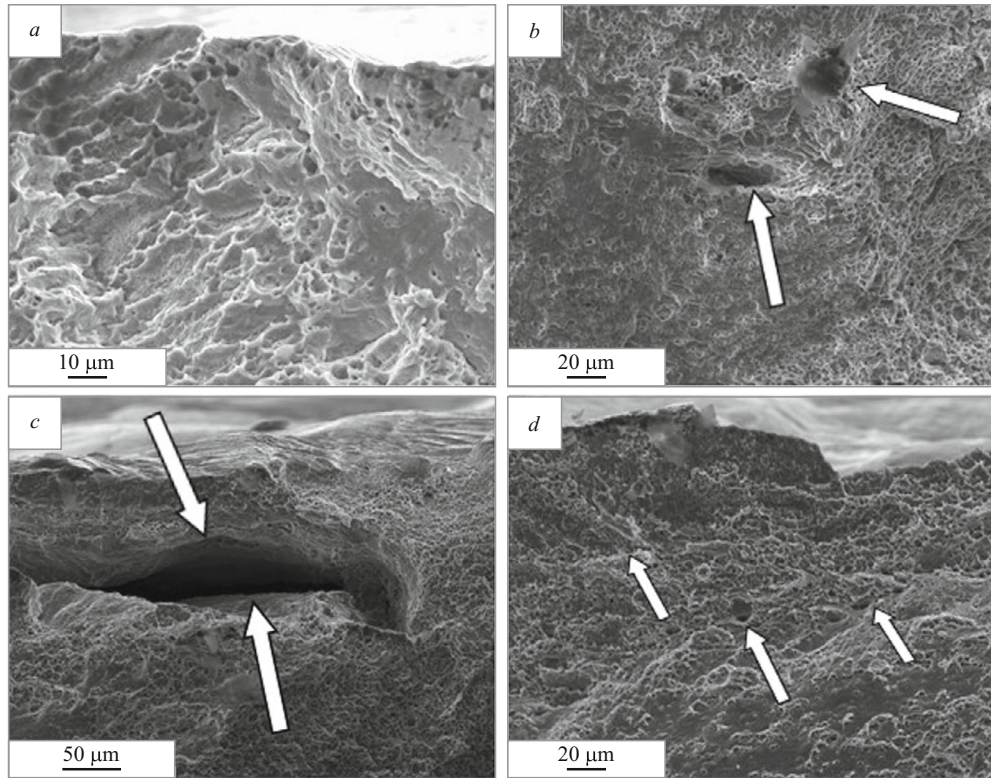


**Fig. 2.** Fracture surface of a high-entropy Cr – Mn – Fe – Co – Ni alloy in the initial state: *a*) viscous pit fracture; *b, c, d*) micropores, micro-layers and layered arrangement of micropores, respectively (shown by arrows).

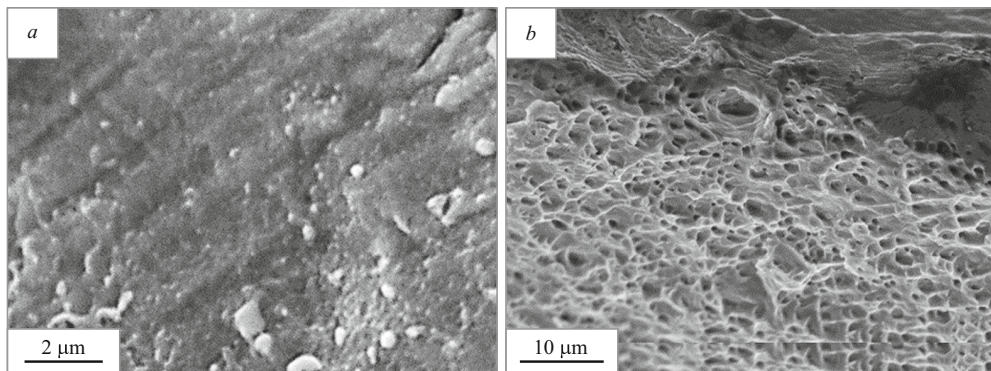


**Fig. 3.** Fracture surface of a high-entropy Cr – Mn – Fe – Co – Ni alloy after irradiation with a pulsed electron beam at  $E_s = 30 \text{ J/cm}^2$  and tensile testing: *a*) in the destruction band; *b*) out of the band.

pores, micro-layers and voids in the material (Fig. 2*b* and *c*). These material defects are very often located in the fracture in the form of extended strips (Fig. 2*d*). It can be assumed that this distribution of defects is due to the peculiarities of manufacturing bulk material.

Two-way irradiation of the working surface of the samples prepared for tensile testing leads to a decrease in the strength and plastic properties of the HEA. Along with areas destroyed by a viscous mechanism, studies of the fracture surface of samples after EBI revealed sections of the material

in which a banded (lamellar) fracture structure is formed during the destruction process (Fig. 3).

In most cases, the fracture bands, which intersect the fracture of the sample from its upper to lower edge, are located at an angle of 90 or 45° to the surface of the sample. The destruction of the sample in such bands proceeds by a viscous mechanism. The diameter of the separation pits in the fracture bands varies within 0.1 – 0.2 μm, which is almost an order of magnitude smaller than the diameter of the viscous separation pits in the rest of the sample.

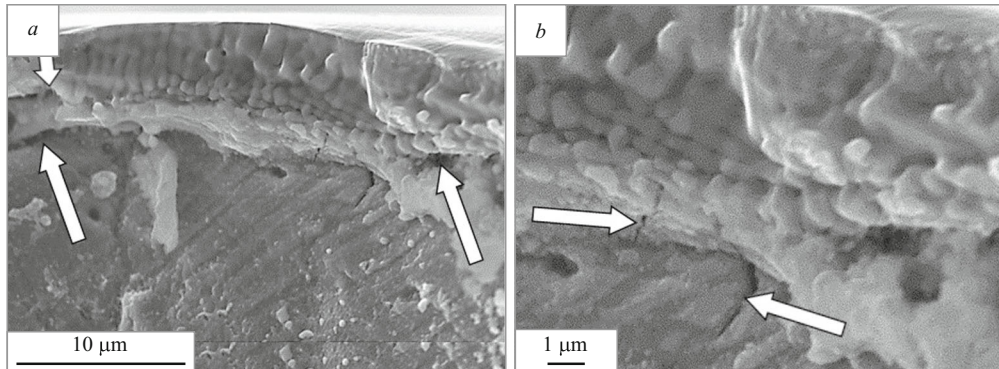


**Fig. 4.** Structure of high-speed cellular crystallization in the fracture of the surface layer of a high-entropy Cr – Mn – Fe – Co – Ni alloy after irradiation with a pulsed electron beam at  $E_s = 30 \text{ J/cm}^2$  (arrows show micropores).

The conducted studies show that destruction bands do not form in a sample not irradiated by a pulsed electron beam. The size of the region of the material whose destruction took place with the formation of the band structure of the fracture increases with an increase in the energy density of the electron beam. Thus, at  $E_s = 10$  and  $30 \text{ J/cm}^2$ , the regions with a band structure of the fracture occupy  $\approx 25$  and  $\approx 65\%$  of the total fracture area, respectively. The formation of the band structure of the fracture during the destruction of the HEA can be assumed to be one of the reasons for the decrease in the strength and ductility characteristics of the material in the irradiated state.

In general, irradiation of metals and alloys with a pulsed electron beam leads to the formation of a high-speed cellular crystallization structure in the surface layer of the sample (Fig. 4a). It is established that the average size of crystallization cells, which depends on the electron beam energy density, increases from  $310 \text{ nm}$  at  $E_s = 15 \text{ J/cm}^2$  to  $800 \text{ nm}$  at  $E_s = 30 \text{ J/cm}^2$ . When irradiated with  $E_s = 10 \text{ J/cm}^2$ , the surface layer of the HEA does not melt.

By studying the fracture surface of the HEA samples it was possible to estimate the thickness of the molten layer and consider the state of the boundary (melt/solid) layer formed during high-speed crystallization of the material, realized as a result of irradiation with a pulsed electron beam. The studies showed that the thickness of the molten layer increases from  $0.8$  to  $5 \mu\text{m}$  with an increase in the energy density of the electron beam.

The sizes of the crystallites of the layer are almost identical to the sizes of the crystallization cells discussed above. The bulk of the HEA modified by the electron beam has a two-layer structure. Micropores are located at the interface of the surface and subsurface layers, as well as the subsurface layer and the base metal (Fig. 4a). The subsurface layer and the adjacent volume of the base metal contain microfractures mainly located perpendicular to the surface of the sample (Fig. 4b). However, no such fractures were found in the surface layer. It can be assumed that the defects identified in

these layers are formed as a result of elastic stresses arising during high-speed quenching of samples after thermal exposure to an electron beam, i.e., the defective substructure of the HEA is thermally unstable, which leads to a decrease in its mechanical properties.

## CONCLUSIONS

The results of studies into a high-entropy alloy of the Co – Cr – Fe – Mn – Ni system following electron beam irradiation (EBI) with an energy density of  $10 - 30 \text{ J/cm}^2$  can be used to determine the influence of EBI on the mechanical properties and structure of the alloy.

Destruction of the initial and irradiated samples of the HEA during tensile tests proceeds according to a viscous mechanism. It is shown that irradiation leads to a decrease in the characteristics of the strength and flatness of the HEA, which increases with the growth of the energy density of the electron beam. The destruction of a HEA previously irradiated by a pulsed electron beam was shown to be accompanied by the formation of a band-fracture structure. The destruction surface area of the irradiated samples occupied by the band structure increases with an increase in the energy density of the electron beam. The study of the fracture surface revealed that the thickness of the molten layer, which varies from  $0.8$  to  $5 \mu\text{m}$ , increases with an increase in the energy density of the electron beam.

*This work was supported by the Russian Foundation for Basic Research (project No. 20-19-00452).*

## REFERENCES

1. E. P. George, W. A. Curtin, and C. C. Tasan, "High entropy alloys: A focused review of mechanical properties and deformation mechanisms," *Acta Mater.*, **188**, 435 – 474 (2020).
2. V. Shivam, J. Basu, V. K. Pandey, et al., "Alloying behaviour, thermal stability and phase evolution in quinary AlCoCrFeNi high entropy alloy," *Adv. Powd. Tech.*, **29**, 2221 – 2230 (2018).

3. U. L. Ganesh and H. Raghavendra, "Review on the transition from conventional to multi-component-based nano-high-entropy alloys-NHEAs," *J. Therm. Anal. Calor.*, **139**, 207 – 216 (2020).
4. Y. A. Alshataif, S. Sivasankaran, F. A. Al-Mufadi, et al., "Manufacturing methods, microstructural and mechanical properties evolutions of high-entropy alloy: a review," *Met. Mater. Intern.*, **26**, 1099 – 1133 (2019).
5. K. C. Cheng, J. H. Chen, S. Stadler, and S. H. Chen, "Properties of atomized AlCoCrFeNi high-entropy alloy powders and their phase-adjustable coatings prepared via plasma spray process," *Appl. Surf. Sci.*, **478**, 478 – 486 (2019).
6. J. Joseph, P. Hodgson, T. Jarvis, et al., "Effect of hot isostatic pressing on the microstructure and mechanical properties of additive manufactured Al<sub>x</sub>CoCrFeNi high entropy alloys," *Mater. Sci. Eng. A*, **733**, 59 – 70 (2018).
7. R. Jian, L. Wang, S. Zhou, et al., "Achieving fine-grain tungsten heavy alloys by selecting a high entropy alloy matrix with low W grain growth rate," *Mater. Lett.*, **278**, 128405 (2020).
8. V. E. Gromov, S. V. Konovalov, Yu. F. Ivanov, and K. A. Osintsev, "Structure and properties of high-entropy alloys," *Adv. Struct. Mater.*, **107**, 110 (2021).
9. A. A. Rempel and B. R. Gelchinsky, "High-entropy alloys: obtaining, properties, practical application," *Chern. Metall.*, **63**(3 – 4), 248 – 253 (2020).
10. A. S. Rogachev, "Structure, stability, and properties of high-entropy alloys," *Fiz. Met. Metalloved.*, **121**, 807 – 841 (2020).
11. V. F. Bashev and A. I. Kushnerev, "Structure and properties of cast and liquid-quenched high-entropy alloys of the Al – Cu – Fe – Ni – Si system," *Fiz. Met. Metalloved.*, **118**(1), 42 – 50 (2017).
12. D. G. Shaisultanov, N. D. Stepanov, G. A. Salishchev, and M. A. Tikhonovskii, "Effect of heat treatment on the structure and hardness of high-entropy alloys CoCrFeNiMnV<sub>x</sub> (X = 0.25, 0.5, 0.75, 1)," *Fiz. Met. Metalloved.*, **118**(6), 610 – 621 (2017).
13. T. Zhang, L. Xin, F. Wu, et al., "Microstructure and mechanical of Fe<sub>x</sub>CoCrNiMn high-entropy alloys," *J. Mater. Sci. Technol.*, **35**(10), 2331 – 2335 (2019).
14. B. A. Gludovatz, A. Hohenwarter, and D. Catoor, et al., "Fracture-resistant high-entropy alloy for cryogenic applications," *Science*, **345**(6201), 1153 – 1158 (2014).
15. D. I. Proskirovsky, V. P. Rotshtein, G. E. Ozur, et al., "Physical foundations for surface treatment of materials with low energy, high current electron beams," *Surf. Coat. Technol.*, **125**(1 – 3), 49 – 56 (2000).
16. S. Konovalov, Y. Ivanov, V. Gromov, and I. Panchenko, "Fatigue-induced evolution of AISI 310S steel microstructure after electron beam treatment," *Materials*, **13**(20), 4567 (2020).
17. K. Osintsev, V. Gromov, Y. Ivanov, et al., "Evolution of structure in AlCoCrFeNi high-entropy alloy irradiated by a pulsed electron beam," *Metals*, **11**, 1228 (2021).
18. *GOST 1497–84. Metals. Tensile Test Methods* [in Russian], Moscow, Standartinform (2005).
19. N. N. Koval and Yu. F. Ivanov, "Nanostructuring of the surface of metal-ceramic and ceramic materials during pulsed electron-beam processing," *Izv. Vysh. Uchebn. Zaved., Fizika*, No. 5, 60 – 70 (2008).